# Evaluation of Impact Energy Attenuators and Composite Material Designs of a UAM VTOL Concept Vehicle

Jacob Putnam
Jacob.B.Putnam@nasa.gov
Research Aerospace Engineer
NASA Langley Research Center
Hampton VA, 23681

Justin Littell
Justin.D.Littell@nasa.gov
Research Aerospace Engineer
NASA Langley Research Center
Hampton VA, 23681

## ABSTRACT

The development of Vertical Take-off and Landing (VTOL) vehicles for the Urban Air Mobility (UAM) markets presents a need for light weight vehicle structures with effective occupant protection capabilities. The National Aeronautics and Space Administration (NASA) has been working to fill that need, recently developing a cadre of concept vehicles to help characterize UAM design feasibility. This paper describes a study, using these concept vehicles, to evaluate the use of advanced composite structure and energy attenuating designs in the UAM vehicle design space. A finite element model (FEM) of a single passenger quadrotor concept vehicle was developed in LS-Dyna® and simulated under nominal and off-nominal vertical impact conditions. A variety of energy attenuating design mechanisms were implemented within this model to quantify their effectiveness in improving occupant safety. The use of carbon composites in both the energy attenuation mechanisms and vehicle structure was evaluated. The results of this study found significant reduction in occupant injury risk with the implementation of energy absorbing composite crush tubes and landing gear within the vehicle design. Additionally the use of a carbon fiber as a structural material was found to provide significant weight reduction while maintaining similar occupant loads to that predicted with an aluminum structure. This work provides a preliminary evaluation of design mechanisms and materials that may be used to optimize occupant protection capabilities within the UAM market.

## INTRODUCTION

The emergent stage of any new technological capability is vital to defining how the public interacts with and perceives that technology. The emergence of electric Vertical Take-off and Landing (eVTOL) vehicles is no exception. This technology has the ability to revolutionize the field of public and private aerospace transportation by opening up the untapped market of short distance aerospace transportation, particularly for the urban environment. Coined "Urban Air Mobility," there is a technological race to fill this new market space amongst aerospace industry stalwarts and startups. During the early stages of this developing marketplace, there is a unique opportunity to shape design priorities and regulations prior to widespread design development and implementation.

The eVTOL vehicle presents a variety of new design constraints and opportunities. Vehicle size and weight are two of the most significant constraints. Size restrictions are required to harbor and transport these vehicles within population-dense areas. Limitations in electric propulsion and use of existing infrastructure for operations constrain vehicle weight. These constraints have been driving the development of eVTOL vehicles towards advanced lightweight materials with particular interest in carbon fiber composites. Other design considerations include features such as autonomous operation, redundant sources of lift, and distributed power systems.

With these new constraints comes the opportunity to rethink establish considerations for occupant protection early in the design life cycle. In past evolutions of transportation technology, occupant protection had not been at the forefront of design until well after the initial design paradigms have been set. For example, the first commercial airplanes began operation in 1914, it wasn't until 44 years later that the

*Presented at the VFS 75th Annual Forum and Technology Display, May 13-16, 2019, Philadelphia, Pennsylvania.*

Federal Aviation Administration (FAA) was formed to develop and enforce occupant safety standards. In the automotive world, the National Highway Safety Administration (NHTSA) was not established until 1970, 62 years after the first Model T came off the production line. These governing bodies have been founded due to the necessity for standardization in rules for safety in vehicle design and operation required by the public.

Both the automotive and aviation industries have developed tools to improve occupant safety in design. One of the most significant tools has been the development of the Anthropomorphic Test Device (ATD), more commonly referred to as a crash test dummy [1]. ATD's have allowed standardization of injury risk prediction, providing means to quantitatively optimize vehicle design for occupant protection through vehicle testing. This has led in the development of multiple approaches used to reduce injury and death during mishaps. These approaches either restrain occupant motion, seatbelts and airbags, or absorb energy, crumple zones and stroking seats.

Design optimization and development through ATD testing has proven effective. However the cost and time involved in conducting many of these tests restrict their applicability, particularly early in the design lifecycle. Computational finite element analysis (FEA) codes such as LS-DYNA® [2] are often used to fill these knowledge gaps.

The National Aeronautics and Space Administration (NASA) has continually worked to develop capabilities within LS-DYNA® to predict the response of aerospace vehicular structures and occupants under dynamic loading conditions. This work has ranged from simulating an expansive range of aerospace vehicle tests with ATDs to the development, calibration, and verification of advanced composite material models [3-5]. This has resulted in a toolkit for evaluating aircraft designs with regards to their occupant protection capabilities. This study leverages these tools to provide an assessment of occupant protection capabilities within eVTOL vehicles, in particular of available mechanisms and materials that can be used to advance them.

With the goal of focusing NASA's research in support of VTOL aircraft development, a group of researchers at NASA Ames Research Center recently developed a cadre of conceptual eVTOL vehicles [6,7]. These design concepts include a single passenger electric, six passenger hybrid, and a fifteen passenger turbo-electric vehicle intended to cover the range of payload, range, and propulsion types expected within the current UAM design space. Of these the single passenger configuration and simple airframe shape made the electric quadrotor concept ideal for further evaluation of occupant protection capabilities.

In this study, the single passenger quadrotor concept is expanded upon. The occupant and structural analysis tools previously developed are implemented within the design to assess its airworthiness potential. This work provides an early look into the value of focused design optimization to shape occupant safety in the UAM market.

## METHODS

### NASA Concept Vehicle

To evaluate the single passenger quadrotor design concept, a finite element model (FEM) of the vehicle structure first had to be developed. To assist in this a computer aided design (CAD) model of the quadrotor was provided by NASA Ames [6] (Figure 1). This CAD model was then de-featured and the outer shell was meshed using approximately 2x2-in. quadrilateral shell elements in Hypermesh® 14.0 [8]. After developing the FE mesh, the FEM was imported into LS-DYNA® where it was further defined. Nonstructural vehicle components such as the rotor group, drive train, and batteries were replaced with point masses rigidly fixed to the vehicle structure using constrained nodal rigid bodies (CNRB's). Component masses were set based on vehicle design specifications. The developed structural model consisted of: 9,234 nodes, 9,265 shell elements, 3 parts, and 10 concentrated masses. The total weight of the structural model (w/ aluminum airframe) was 1,308 lb., this weight was 56 lb. over the estimated design weight of 1,252 lb.

**Figure 1. NASA single passenger quadrotor design concept (left), CAD (middle), and FEM (right)**

To evaluate the use of advanced composites on new UAM airframe designs, three unique airframe (wings, fuselage, and landing struts) material models were implemented. In addition to the traditional aluminum

airframe two carbon composite materials were evaluated. The first was a carbon fiber plain weave with 3k-sized carbon tows in the warp and fill directions, designated as C/C. The second was of a hybrid composite consisting of plain 3k-sized carbon fiber in the warp and 3k-sized aramid fibers in the fill direction, designated as C/A. The composite material densities were approximately half that of the traditional aluminum material, and so provide a weight savings if used as a direct replacement. The evaluation of these composite materials in this study provided an understanding of the trade between weight reduction and occupant safety.

The baseline aluminum material was modeled within LS-DYNA® using *MAT_003 for aluminum 7075-T73 previously verified against commercial aircraft fuselage section tests [9]. All elements were modeled using single point integration (Hughes-Liu). The shell wall thickness of each aluminum airframe component was 0.05 in. for fuselage, 0.1 in. for wings, and 0.25 in. for landing struts.

The C/C and C/A material definitions implemented in this model were characterized, calibrated, and verified through a series of building block studies carried out at NASA LaRC [5]. The crush response of the material was verified against dynamic impact tests of composite tubes [10]. The developed material parameters (Table 1) were implemented using *MAT_058 in LS-DYNA®. Each component was modeled as a 45° oriented 4-ply layup, defined using *PART_COMPOSITE. All elements were defined using single point integration (Hughes-Liu) with viscous hourglass control. The total shell wall thickness of each composite component matched that of the aluminum airframe.

**Table 1. Defined Material Properties of Carbon Composites Models**

| | C/C Material | C/A Material |
|---|---|---|
| RO, lb.-s$^2$/in.$^2$ | 1.29E-4 | 1.29E-4 |
| EA, psi | 6.5E+6 | 6.3E+6 |
| EB, psi | 6.5E+6 | 2.76E+6 |
| PRBA | 0.1095 | 0.1095 |
| TAU1, psi | 7.94E+3 | 4.50E+3 |
| GAMMA1, in/in | 0.0246 | 0.0246 |
| GAB, psi | 3.0E+5 | 3.0E+5 |
| SLIMT1 | 0.8 | 0.8 |
| SLIMC1 | 1.0 | 1.0 |
| SLIMT2 | 0.8 | 0.8 |
| SLIMC2 | 1.0 | 1.0 |
| SLIMS | 1.0 | 1.0 |
| AOPT | N/A* | N/A* |
| ERODS | 0.5 | 0.5 |
| FS | -1 | -1 |
| A1,A2,A3 | N/A* | N/A* |
| D1,D2,D3 | N/A* | N/A* |
| E11C, in/in | 0.011 | 0.013 |
| E11T, in/in | 0.0143 | 0.0143 |
| E22C, in/in | 0.011 | 0.025 |
| E22T, in/in | 0.0143 | 0.025 |
| GMS, in/in | 0.142 | 0.142 |
| XC, psi | 7.00E+4 | 7.00E+4 |
| XT, psi | 8.90E+4 | 8.90E+4 |
| YX, psi | 7.00E+4 | 5.00E+4 |
| YT, psi | 8.90E+4 | 5.40E+4 |
| SC, psi | 7.10E+3 | 7.10E+3 |

**AOPT parameter not used as ply direction defined in PART_COMPOSITE.*

Occupant Protection Mechanisms

To evaluate occupant loading, a seat and rigid floor were modeled within the base vehicle airframe. The seat was developed from a public sourced CAD of a carbon fiber racing seat [11]. The CAD was defeatured and converted to a FE mesh using Hypermesh® 14.0. The seat material was defined within LS-DYNA as 4-ply 0.06-in. thick layers of the C/C material. The floor was modeled as a 0.13-in. thick rigid shell placed at the approximate occupant foot height. Connections between the airframe, floor, and seat were assumed rigid. These rigid connections provided a conservative baseline to assess component additions against. To predict occupant loads, a mid-size male occupant was modeled using the LSTC Hybrid III 50$^{th}$ Automotive ATD FEM version 151214_BETA [12]. Although the Hybrid III automotive configuration has a curved spine and does not meet FAA specifications for lumbar load analysis, this model was used as a preliminary tool to quantify loads as it is the only publicly available mid-size Hybrid III FEM. The ATD was positioned within the seat in an upright 90° knee – 90° hip posture. The lumbar spine was partially straightened to achieve this position using the lumbar rotation operation within LS-PrePost®. A 5-point seat belt was modeled to restrain the occupant during landing. The model consisted of mixed shell and 1-D seatbelt elements fit around the ATD. Material property definitions of the belt were taken from a previously developed and verified 5-point belt model [13]. This base occupant system consisted of: 295,159 nodes, 245,464 shell elements, 225,602 solid elements, 383 parts, and 10 concentrated masses

(Figure 2). The occupant model (ATD, seat, floor, and belts) weighed a total of 206 lb.

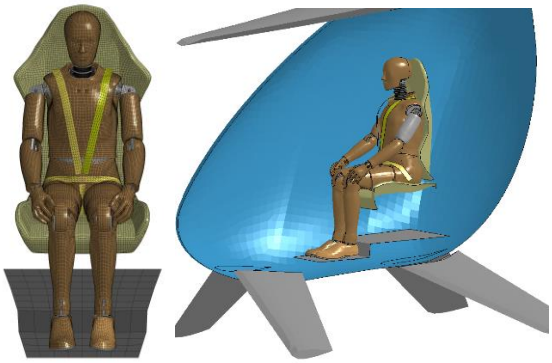

**Figure 2. Occupant Model**

Individual energy attenuating components were implemented in the model using a "pyramid approach". Each implemented component was stacked upon the previous. Thus the last configuration evaluated included all components. The first implemented component was a subfloor which provided compliance between the floor and the vehicle airframe (Figure 3). This component consisted of 3 semi-ellipse shell pieces running the width of the airframe. Each shell section had a thickness of 1/16-in. and was modeled in the respective material type of the vehicle structure evaluated. In the aluminum form this component weighed a total of 1.9 lb., while the composite form weighed 1 lb. This weight improvement is due to the lower mass density of the composite material. Geometry was not altered between the subfloors.

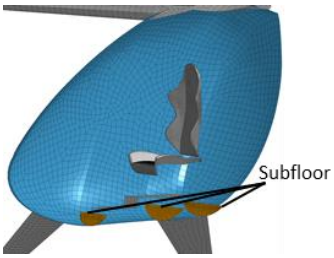


Weight: 1.0-1.9 lb

**Figure 3. Model of subfloor component**

A seat cushion was next added to the seat. This cushion included seat pan and seat back components (Figure 4). Seat pan consisted of two foam layers, an upper 0.2-in. thick polyurethane and 1.0-in. thick lower polyethylene layer. The seat back foam consisted of one 0.6-in. layer of polyethylene material. This foam setup was modeled after previously tested and modeled commercial aircraft seat cushions [9]. Mat_001 was used to model the polyurethane material, while Mat_057 was used for the thicker polyethylene layer. The complete seat cushion model contained 9904 constant stress solid elements, weighing a total of 1 lb.

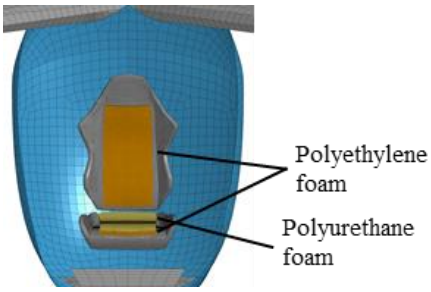


Weight: 1.0 lb

**Figure 4. Model of seat foam component**

To reduce energy transferred into the seat upon impact a single C/A crush tube component was modeled between the rigid floor and seat (Figure 5). The crush tube was of 3-in diameter and 7.8-in. height with four 0.012-in. ply layers. The crush tube was of an accordion shape [10] where it was shown to produce a robust and consistent crush response across varied axis loading conditions. The material definition, element formulation, and composite layup were defined similarly to the C/A airframe. As the seat substructure was not included in the model, a sliding joint was implemented between the seat and floor to approximate the stability it would provide during impact.

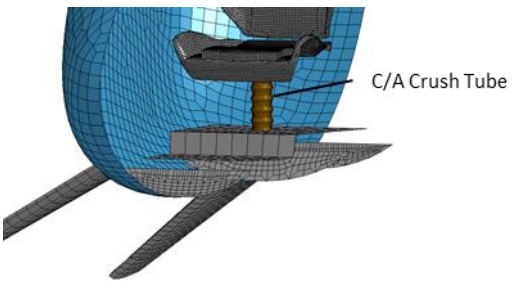


Weight: 0.22 lb

**Figure 5. Model of seat crush tube component**

The conceptual landing struts were next replaced with a more traditional small rotorcraft skid gear, modeled after a MD-500 helicopter design [14]. The skid gear was modeled using C/C tube sections with diameter of 3 in. and shell wall thickness consisting of 4-ply layers at 0.063 in. (Figure 6). The material definition,

element formulation, and composite layup were defined similarly to the C/C airframe. The landing gear was rigidly fixed to an additional subfloor section modeled across the length of the original subfloor. This component ended up weighing less than the original landing struts due to a reduction in material thickness required to provide landing stability.

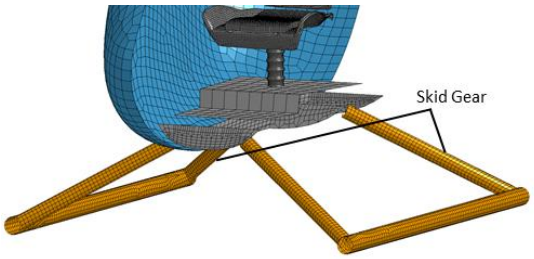


Weight: -23.5 lb
***** Skid gear weight presented as difference from original landing struts

**Figure 6. C/C Skid Gear Model**

Lastly four additional C/A crush tubes were implemented across the airframe to attenuate the energy taken by the landing gear during impact (**Error! Not a valid bookmark self-reference.**). Each tube fixed with a rotational joint was pinned to the airframe at one end and the skid gear strut on the other. This allowed the tubes to rotate with the movement of the struts and limit shear loading of the tubes. These tubes were reduced in height compared to the seat crush tube at 5in., but matched in every other modeled aspect.

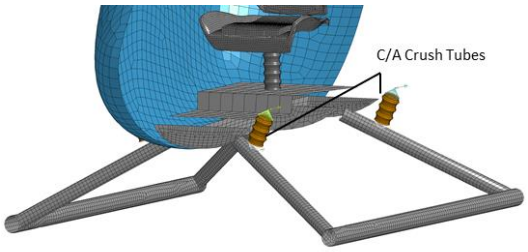


Weight: 0.67 lb

**Figure 7. Skid Gear w/ C/A Crush Tubes Model**

Simulation Methodology

Each design configuration was simulated in a nominal and off-nominal landing condition. In both conditions the vehicle model was impacted against a concrete landing strip (176-in. length, 96-in. width, 8-in. depth) with a set vertical velocity for each case. The nominal velocity was set to 5 ft/s, representative of a free-fall from approximately 6 in. Nominal landing was simulated to insure the vehicle design would not undergo permanent damage at what could be expected for normal operation. Off nominal velocity was set to 30 ft/s or a 14-ft freefall. This impact velocity is recommended by the FAA for vehicle certification due to a high occupant-survival rate collected from experimental and crash data taken on transport-category airplanes at these conditions [1515].

Prior to the impact event, gravitational acceleration was applied to vehicle and occupant for 200 ms. A sensitivity study was carried out to determine this time of pre-load as the minimum for the occupant to reach a steady state load against the seat. During the pre-load phase the belts were tightened to a steady load of 5-lb using a retractor and pretensioner element combination. The vehicle was constrained during this time by a *BOUNDARY_SPC set placed on the rotors represented by nodal masses.

A total of 36 simulations - 3 airframes x 6 configurations x 2 conditions - were performed using LS-DYNA SMP Version R10.1.0 single precision. Simulations were run using 4-8 processors on a Linux computer cluster. Simulations were executed to 0.4-s, with an average CPU run time of approximately 100 hrs.

Output requests for each simulation included the acceleration time history of the vehicle drive train, console, and battery component representative masses. In addition, all ATD model outputs were recorded. ATD upper-neck and lumber spine load cell outputs were post processed after each run to calculate occupant injury risk.

Injury Metrics

To quantify occupant injury risk in each landing scenario and vehicle configuration, two standardized ATD injury metrics were used: peak compressive lumbar load and upper neck injury criteria (Nij). Peak compressive load is the standard ATD injury metric criteria used by the FAA to assess commercial aircraft [16]. This metric evaluates risk of vertebral fracture within the lumbar spine and is calculated as the maximum compressive load measured in the lumbar spine load cell during test. The FAA limit for seat certification is 1500 lbs. for the 50$^{th}$ male ATD. Nij is used by the NHTSA in the certification of new vehicles [1717]. Nij predicts risk of injury to the upper cervical spine and is calculated as a combination of axial loading and bending moment measured in the

upper neck load cell. NASA has adopted both of these metrics for occupant protection analysis [18].

## RESULTS

Vehicle data was filtered according to SAE-J211 [1919] recommendations. The ATD output was filtered according to LSTC recommendations for the Hybrid III FEM [1217]. Calculated lumber spine compressive load for each simulated configuration under off-nominal loading is provided below in Table 2.

**Table 2. Lumbar load response calculated under off-nominal loading**

| Configuration | Al Airframe | C/C Airframe | C/A Airframe |
|---|---|---|---|
| Baseline | 5758.7 lb | 6194.6 lb | 6426.1 lb |
| Add Subfloor | 3889.8 lb | 4022.5 lb | 3741.6 lb |
| Add Seat Foam | 3323.6 lb | 3430.7 lb | 3268.2 lb |
| Add Seat Level C/A Crush Tube | 1533.3 lb | 1801.8 lb | 1868.9 lb |
| Add C/C Skid Gear | 905.2 lb | 983.7 lb | 1315.3 1b |
| Add C/A Crush Tubes to Skid Gear | 1019.0 lb | 1211.9 lb | 1172.1 lb |

The predicted lumbar load shows a progressive decrease in occupant injury risk with each component addition. The greatest decreases in occupant injury risk are seen with the addition of the Subfloor, Seat Crush Tube, and Skid gear. The upper neck injury risk calculated through the Nij metric (Table 3) similarly matched the trends observed in the lumbar load metric. This finding is to be expected as the primary load path is vertical through the lumbar spine up into the neck. Similarities in response between these metrics across design cases provides assurance that the evaluated design features did not induce significant off-axis loading on the occupant during impact. To simplify discussion occupant risk response will be primarily referred in terms of lumbar load throughout the rest of this paper.

**Table 3. Nij response calculated under off-nominal loading**

| Configuration | Al Airframe | C/C Airframe | C/A Airframe |
|---|---|---|---|
| Baseline | 1.2 | 1.14 | 1.30 |
| Add Subfloor | 0.75 | 0.72 | 0.74 |
| Add Seat Foam | 0.67 | 0.72 | 0.66 |
| Add Seat Level C/A Crush Tube | 0.23 | 0.43 | 0.41 |
| Add C/C Skid Gear | 0.20 | 0.17 | 0.26 |
| Add C/A Crush Tubes to Skid Gear | 0.19 | 0.19 | 0.25 |

Airframe Material differences

In general, the stiffer airframe structure materials were found to produce lower occupant loads (Figure 8). Though slight, the difference between the three airframe materials was consistent. The C/A airframe did exhibit lower loads with the addition of the subfloor, but this is due to added compliance in that mechanism with this material. It is likely that both the Aluminum and C/C airframes would exhibit lower loads with subfloors built of the C/A material rather than their respective structural materials. These results indicate that a direct substitution of composite material for metallic does not always improve the crashworthiness of the vehicle and designs must be optimized to take advantage of the composite material features.

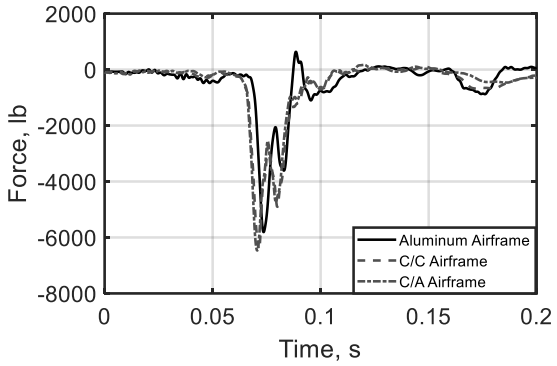


**Figure 8. Lumbar load comparison between base airframe material models**

Subfloor

The composite subfloor was shown to significantly reduced occupant loading across designs by up to 42%. Upon impact, the subfloor crumpled both absorbing energy and distributing the deceleration impulse over a longer period of time. The composite subfloors provided a greater reduction in occupant loading than aluminum, with the more compliant C/A subfloor providing the greatest reduction (Figure 9).

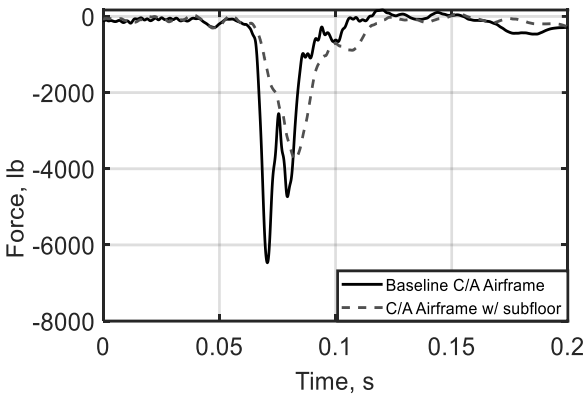


**Figure 9. Lumbar load change due to implementation of subfloor in the C/A vehicle**

Foam padding on seat

The addition of foam padding between seat and occupant resulted in a minimal improvement in all three airframe designs. Other than providing comfort to the occupants these results suggest that seat padding is not the tool to drive changes in occupant loading. However, there is value in evaluating the effects of foam on occupant response, in certain conditions padding can increase occupant loading by increasing the velocity differential between occupant and seat at impact [18].

Seat Crush Tube

The C/A crush tube implemented between the seat and floor was found to be the most effective component to reduce occupant injury risk. This component reduced the lumbar load by more than half during impact in the aluminum airframe. The crush tube distributed the impact energy over multiple pulses (Figure 10). The first consisted of the initial buildup to crush load in the tube followed by crush. The load oscillated during crush and then peaked when the tube bottomed out against the floor. The peak load and response shape could be further optimized through adjustments to size, geometry, and number of composite ply layers used.

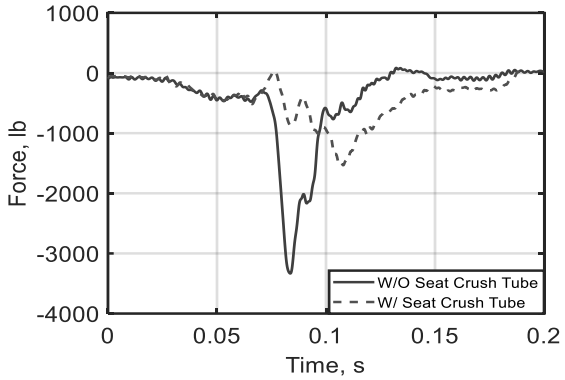


**Figure 10. Lumbar load change due to implementation of composite crush tube within seat design in the Aluminum vehicle**

Composite Skid Gear

The use of composite tube skid gear fixed to the vehicle subfloor also significantly reduced occupant injury risk. The composite skid gear reduced peak loading by absorbing energy on initial impact (Figure 11). The composite skid gear exhibited greater rigidity than the original gear allowing it to slow down the vehicle by absorbing energy through bending and minor crushing of the C/C tubes, preventing the fuselage from contacting the ground. Remaining energy was taken out through the seat crush tube which did not bottom out in this configuration. With this component the total lumbar loading was decreased in all vehicles by a factor greater than 5 from original and shown to be well within currently defined limit of 1500 lbs.

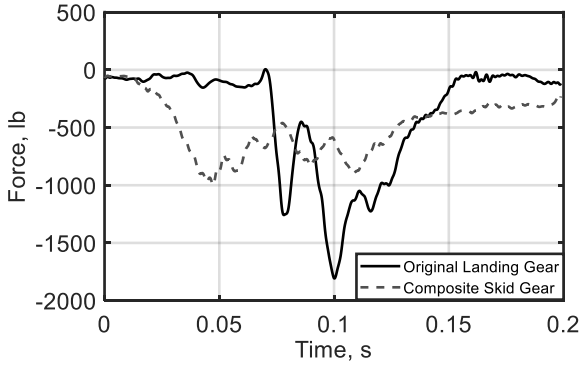


**Figure 11. Lumbar load change due to implementation of M-500 composite skid gear in the C/C vehicle**

Skid Gear w/ Crush Tubes

The addition of C/A tubes to each skid gear strut was shown to reduce the load transferred through the skid

gear to the occupant but did not reduce total occupant loading in all vehicles (Figure 12). The C/A tubes were effective at controlling the bending and failure of the skid gear struts. The tubes only allowed the struts to bend and fail after their crush initiation load had been reached. At this point, the combined energy absorption of the tubes and struts pulled out a significant portion of energy from the system while reducing the strut damage observed in prior simulation. This reduced lumbar loading during this phase of impact but resulted in an increase in total peak lumbar load in both the C/C and aluminum vehicles. It is postulated that the energy taken out of the system by the skid crush tubes reduced the effectiveness of seat level crush tubes. In this configuration the seat crush tube did not completely crush, absorbing less energy in this phase of impact. At these lower energies the slight reduction in energy attenuation is reasonable as these components are individually tuned to reduce loads to sub-injurious levels while retaining rigidity in low energy impacts.

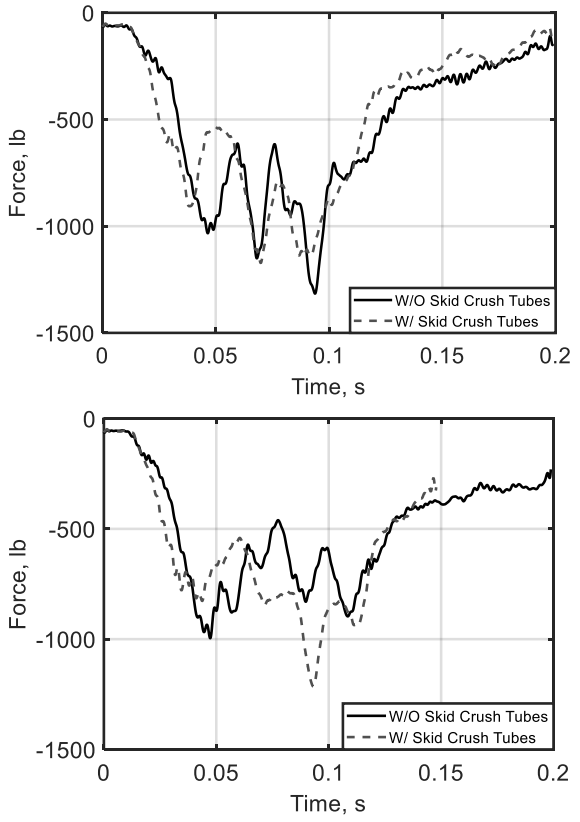


**Figure 12. Lumbar load change due to implementation crush tubes in composite skid gear in the C/A (top) & C/C airframe (bottom)**

Baseline vs Final Vehicle Design

From the baseline configuration to the final configuration with all implemented occupant protection mechanisms, the lumbar load experienced by the occupant was reduced by approximately 81%. In addition to improving occupant response, the implementation of all mechanisms reduced vehicle weight by 20 lb. This reduction was primarily due to the implementation of lighter weight skid gear. A total weight reduction of 169 lb was achieved when compairing the base aluminum vehicle and final C/C design. A comparison between the baseline aluminum model and final C/C model at peak impact load is shown in Figure 13. The energy absorption through material compliance and crushing can be seen in the signficantly higher deformations observed in the final model. Though increased deformation occured, no signficant intrusion into the occupant space was observed. This indicates no increased injury risk due to contact with the vehicle structure.

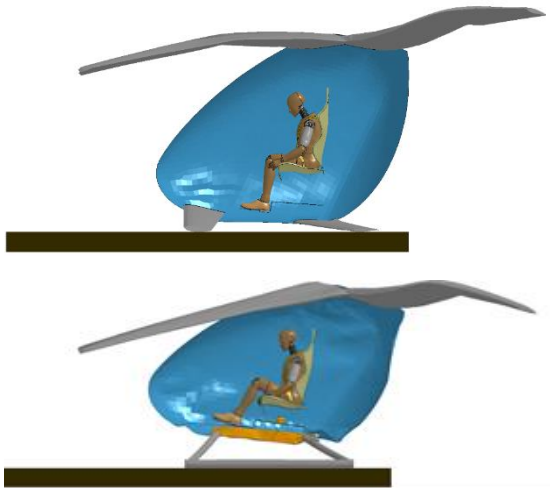

**Figure 13. Peak crush response of the base aluminum vehicle model (top) and the final C/C vehicle model (bottom) under off-nominal loading**

To ensure this greater compliance did not inhibit vehicle effectiveness during nominal vehicle operations the models were qualitatively evaluated for material deformation (Figure 14). No deformation was observed, indicating robustness in the systems evaluated for standard vehicle use. All components also retained rigidity under nominal loading, lending their capability as effective UAM design components.

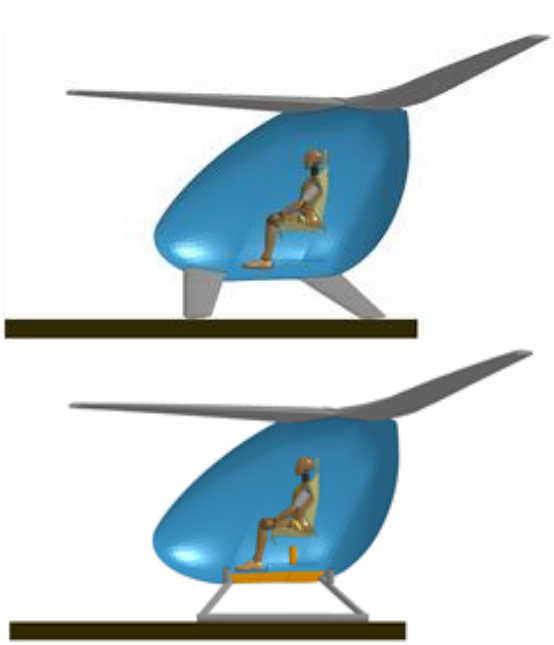

**Figure 14. Peak crush response of the base aluminum vehicle model (top) and the final C/C vehicle model (bottom) under nominal loading**

## CONCLUSIONS

The simulations described in this study were performed to identify the relative effectiveness of various occupant protective mechanisms when applied to an eVTOL vehicle design. Mechanisms were assessed in an off-nominal impact condition representative of a free-fall of 14ft. This condition was selected with the intent to demonstrate the value of an occupant protection design focus to significantly improve survivability.

The mechanisms evaluated in this study were all based on tools currently implemented in aero- and rotorcraft vehicles. The materials used in design included both traditional aluminum and carbon composites. Composites were implemented to demonstrate how these novel materials can be used in conjunction with traditional mechanisms to improve occupant protection design with minimal weight cost.

The use of carbon composite (C/C) for the vehicle structure was shown to significantly reduce vehicle weight while not significantly increasing occupant loads. The C/C vehicle was shown to produce slightly higher occupant loads than the aluminum design in each configuration. Adjustments to the composite layup, such as adding additional ply layers, may bring the occupant response in the C/C vehicle closer to aluminum by increasing overall stiffness while continuing to provide weight reduction. The applicability of the C/C airframe structure was demonstrated in its ability to withstand nominal operating loads without deformation. In this study the greater compliance of the carbon aramid (C/A) material as a structural material was not shown to further improve occupant loading. The increased compliance in this material could drive increased intrusion risk and results indicate limited value in using C/A as a direct replacement for a structural material. As vehicle designs become better defined further studies may evaluate the use of this material in sub-sections of the vehicle structure to optimize performance and safety.

The implementation of occupant protective mechanisms within the evaluated VTOL design were shown to significantly decrease the predicted risk of occupant injury at the off-nominal impact condition. With the implementation of all occupant protective mechanisms, predicted lumbar load went from close to 4 times the prescribed injury limit to close to half. Upper neck injury risk (Nij) was similarly reduced. The implementation of these mechanisms within the design were shown to have minimal weight cost, actually reducing overall weight when replacing the conceptual landing gear with traditional carbon tube struts.

Of the mechanisms implemented, the C/A composite tube, as a stroking mechanism between the seat and floor was found to be the most effective tool for reducing occupant load. Application of a composite crush tube to absorb energy between the seat and vehicle can provide an incredibly versatile tool for reducing occupant loads. The energy absorptive properties can be further tuned through adjustments to the tubes height, radius, and wall thickness. This mechanism also inflicts minimal operational cost, with its low weight and ability for replacement separate from the seat structure.

The implementation of a traditional light rotorcraft landing gear design exhibited increased rigidity over the conceptual design and resulted in a significant decrease in occupant loads. Under the off-nominal landing condition the original landing gear quickly buckled. The sturdier designed skid gear, bent but did not fail and thus was able to reduce the airframe velocity prior to impact with the ground. In addition to improved occupant response, though bulkier, the skid gear provided a weight reduction over the original

design due to its lightweight tubular structure. The reduction in both occupant loading and vehicle weight with this design alteration demonstrates the value of accounting for off-nominal impact events in the early stages of vehicle development.

In this study a handful of previously developed design tools were used to significantly improve the occupant protection capabilities of a conceptual eVTOL vehicle. This work demonstrates the value in considering occupant protection in eVTOL design as the paradigm for these vehicles for use in the UAM field is now being set. As further details become available in eVTOL design, additional work may be performed to better define the integration of these mechanisms within the vehicle. In addition, as the operational space is better defined the full range of possible loading conditions particularly multi-axis loading of the vehicle should be evaluated. The results of these efforts will provide significant value in improving occupant safety and with it public perception of the emerging Urban Air Mobility market.

## AUTHOR CONTACT

Jacob Putnam - Jacob.b.putnam@nasa.gov

Justin Littell - justin.d.littell@nasa.gov

## REFERENCES

1. Backaitis, S.H. and Mertz. H.J. (eds), "Hybrid III: The first human-like crash test dummy." Society of Automotive Engineers, PT-44, Warrendale, PA, 1994.

2. LSTC. “LS-DYNA Theory Manual”. Livermore Software Technology Company, Livermore, CA. July 2017.

3. Jackson, Karen E., and Edwin L. Fasanella. "NASA Langley Research Center Impact Dynamics Research Facility Research Survey." Journal of aircraft 41.3 (2004): 511-522.

4. Polanco, M. A., and J. D. Littell. "Vertical Drop Testing and Simulation of Anthropomorphic Test Devices” Proceedings from the 67th Annual Forum and Technology Display. Virginia Beach, VA, May 3-5, 2011.

5. Jackson, K.E., Fasanella, E.L., and Littell, J.D. “Development of a Continuum Damage Mechanics Material Model of a Graphite-Kevlar ® Hybrid Fabric for Simulation the Impact Response of Energy Absorbing Subfloor Concepts.” Proceedings from the 73rd Annual American Helicopter Society Annual Forum and Technology Display. Fort Worth, TX. May 9-11, 2017.

6. Johnson, W., Silva, C., and Solis, E. “Concept Vehicles for VTOL Air Taxi Operations.” Proceedings from the AHS Technical Conference on Aeromechanics Design for Transformative Vehicle Flight. San Francisco, CA. January 16-19, 2018.

7. Silva, C., Johnson, W., Antcliff, K.R., Patterson, M.D., “VTOL Urban Air Mobility Concept Vehicles for Technology Development”. Proceedings from the 2018 Aviation Technology, Integration, and Operations Conference. Atlanta, GA, June-25-29, 2018.

8. Altair. “Hyperworks 14.0 Manual”, Altair Engineering Inc., Troy, MI, 2018

9. Jackson, Karen E., et al. "Finite Element Simulations of Two Vertical Drop Tests of F-28 Fuselage Sections." NASA/TM-2018-219807, 2018.

10. Littell, J. and Putnam, J., “The Evaluation of Composite Energy Absorbers for use in UAM VTOL Vehicle Impact Attenuation”. Proceedings from the 75th American Helicopter Society Annual Forum and Technology Display. Philadelphia, PA. May 13-16, 2019.

11. Maruzza, H. (2016, February 26). Racing Seat Evo. [Online] Available: https://grabcad.com/library/racing-seat-evo

12. S. Guha, "LSTC_NCAC Hybrid III 50th Dummy Positioning & Post-Processing," ed. LSTC Michigan, 2014.

13. Putnam, J. B., Somers, J.T., Wells, J.A., Perry, C. E., & Untaroiu, C.D.. "Development and evaluation of a finite element model of the THOR

for occupant protection of spaceflight crewmembers." Accident Analysis & Prevention 82 (2015): 244-256.

14. Annett, Martin S. "LS-DYNA analysis of a full-scale helicopter crash test". Proceedings from the 11th International LS-DYNA Users Conference. Detroit, MI. 2010.

15. Federal Register. “Special Conditions: Airbus A350-900 Airplane; Crashworthiness, Emergency Landing Conditions.” Vol 79. No. 43. Friday July 25, 2014.

16. Code of Federal Regulations, Title 14 – CFR Part 25. “Airworthiness Standards: Transport Category Airplanes”, Federal Aviation Administration, Washington, DC, 2018.

17. M. Kleinberger, E. Sun, R. Eppinger, S. Kuppa, and R. Saul, "Development of Improved Injury Criteria for the Assessment of Advanced Automotive Restraint Systems," National Highway Traffic Safety Administration, Washington, DC, 1998.

18. Somers, Jeffrey T., Dustin Gohmert, and James W. Brinkley. "Application of the Brinkley dynamic response criterion to spacecraft transient dynamic events." NASA/TM-2013-217380-REV1, 2017.

19. Society of Automotive Engineers. “Surface Vehicle Recommended Practice: Instrumentation for Impact Test-Part 1-Electronic Instrumentation,” SAE J211-1, 2007.